Tectonic dynamics in the Dinggye region, central part of the Tethys- Himalaya terrane: insights from the 3-D electrical structure

Sheng Jin[1], Yue Sheng[2], Wenbo Wei[3], Gaofeng Ye[4], CUGB MT GROUP[5]
[1]China University of Geosciences, Beijing, 1993010830@cugb.edu.cn
[2] China University of Geosciences, Beijing, sysansiro@126.com
[3] China University of Geosciences, Beijing, wwb5130@cugb.edu.cn
[4] China University of Geosciences, Beijing, ygf@cugb.edu.cn

SUMMARY

The Tethys-Himalaya terrane in the north of the Himalayan orogenic belt is characterized by pervasive extensional structures such as N–S-trending normal rifts and the North Himalayan Gneiss Dome (NHGD). The Dinggye region is located in the central part of the Tethys-Himalaya terrane. The southern segment of the Xainza-Dinggye rift (XDR) and the Mabja Gneiss Dome are distributed in this region. In this work, we generate a new 3-D electrical resistivity model from an array of magnetotelluric data in the Dinggye region and examine it in addition to other electrical resistivity models to the north and east from previous works. By comparing the geophysical models with available geological and geochemical evidence, we find a clear relationship between the electrical resistivity structure, the presence of gneiss domes, north-south-trending normal rifting, and deep plunging subduction which is related to the source of Helium isotopes (crustal or mantle origin). Overall, the results suggest that the southern migration of lithospheric materials likely contributed to the evolution of the rifts in the Tethys-Himalaya terrane, which also may have been influenced by uplifting and cooling of gneiss domes. The models are consistent with tearing of the Indian lithosphere beneath the Xainza-Dinggye rift and other adjacent rifts. Additionally, the difference in the electrical structure related to the Indian crust along the east-west direction likely results from the exhumation of the continental slab, metamorphism in the Tethys-Himalaya terrane, and southern extrusion of materials in the Lhasa terrane.

Keywords: Himalayan orogenic belt; Dinggye region; Electrical structure; material migration; Rift.

INTRODUCTION

The Dinggye region, in the central part of the Himalayan orogenic belt, includes the southern part of the Xainza-Dinggye rift and the Mabja Gneiss Dome with leucogranite cores. Previous studies of gneiss domes in this region report the existence of channel flow processes or tectonic exhumation, in addition to partial melting of orogenic mid-crust. However, the relationship between the crustal migration of materials and the north-south-trending normal rifts remains largely unexplored. In this study, the MT array data distributed in the Dinggye region of the Tethys-Himalaya terrane were processed, analyzed, and modeled to obtain a three-dimensional model of the lithospheric electrical structure. We then combined these models with electrical resistivity models for the region directly to the north (Sheng et al., 2021). The electrical models are interpreted with the help of additional information from geological and geochemical studies. This study investigates the relationship between the electrical structure observed and the evolution of the NHGD and its influence on the N-S-trending normal fault, and further hypothesizes the formation mechanism of the XDR in the Dinggye region. In this way, the study attempts to provide insights on the mechanism of E–W extension in the Himalayan orogenic belt.

Data and method

A data set consisting of 62 MT measurements is used in this study (see Figure 1 for the MT site location). The MT data are used to generate a 3-D electrical model using the ModEM inversion algorithm (Egbert and Kelbert, 2012; Kelbert et al., 2014). According to the geometric mean of the diagonal component of the MT data, the starting model is a uniform 100 Ω·m half space. The model grid has 60 cells in the N-S direction, 87 cells in the E-W direction, and 69 cells in the vertical direction (which included seven air cells in each direction). The horizontal grid has a spacing of 4 km (in both directions) in the core region and 1.5 in the padding region. The thickness of the first layer is 100 m in

the vertical direction and increases by a factor of 1.1 in the core region and 1.5 in the padding region. The 3-D inversion uses the impedance tensor data (four complex components) and tipper data (two complex components). A total of 34 frequency points were used, 6 periods in each decade, logarithmically spaced spaced between 0.01 s and 3000 s. Error floors were set to 5% of the sqrt (|Zxy ∗Zyx|) for Zxy and Zyx components and 10% of the sqrt (|Zxy ∗ Zyx|) for the Zxx and Zyy components of the impedance tensor. An error of 5% on impedance is equivalent to about 10% for the apparent resistivity and 2.86° for the phase. Absolute error floors for the tipper data were set to 0.05 for Tx and Ty components. The normalized root-mean-square (nR.M.S.) misfit of the inversion model was reduced from a starting value of 22.33 to 1.85 after 132 iterations. Both the site-by-site nR.M.S. distribution of each separate 3-D inversion and the total impedance and tippe r misfit of the preferred inverse model to the observational data for some selected MT stations show that the electrical structure is constrained by the MT data. According to the average boundary of the upper and middle crust in the district, the electrical structure shows that the large-scale resistive zones are distributed in the mid-lower crust while some conductive zones are scattered distributed in some areas of the upper crust, marked as C1, C2, C3 and C4 (Figure 2, 3). Furthermore, the upper-crustal conductive zones in the vicinity of the IYS in this study show a good correspondence with the conductive zones in the mid-lower crust in the north of the IYS from the results of Sheng et al. (2021).

Result

The electrical structure shows that the middle-lower crust (depth $\geqslant$ 30km) is charactered by the high resistivity while four conductive zones marked as C1-C4 are distributed at depths of 10-25km in the upper crust. The conductance of the conductive zones C1-C4 is at least 35000S, that is, the bulk conductivity of these conductive zones is more than 2.3 S/m. The relationship of conductivity and melt fraction established by the Archie's law indicates that more than 15% volume of water-bearing melt are needed to interpretate the bulk conductivity of 2.3 S/m, which is correspondence to the result of Chen et al. (2018). The melt fractions that were approximately larger than 5% may reduce the effective viscosity by an order of magnitude (Unsworth et al., 2005). Furthermore, enrichment with aqueous fluids may decrease the viscosity of melts, and, with the volume of melts required, the zones can meet the necessary conditions for the local flow of materials.

Discussion and interpratation

The main research results are obtained as follows.
(1) The southern part of the Xainza-Dinggye rift which is in the Tethys-Himalaya terrane (south of the IYS) resulted from the southern migration of material. The crustal materials in the middle crust of the Lhasa terrane migrated along the Main Himalaya Thrust (MHT) to the upper crust of the Tethys-Himalaya terrane, which could result in the partial melting of the upper crust. This process can decrease the effect viscosity of rocks beneath the Xainza-Dinggye rift and surroundings, which may form the N-S-direction rifts in the background of the E-W-direction extension (Figure 1).
(2) According to the metamorphism and anatexis era (~45Ma-15Ma; King et al., 2011; Yu et al., 2011; Zhang et al., 2018), the conductive zones C3 and C4 may connected with the conductive zones C1 before the Miocene, which indicates a continuous migration of materials in the upper crust of the Tethys-Himalaya terrane. The resistivity of the upper crust beneath the Mabja gneiss dome increase during the cooling process following the evolution and formation of the gneiss dome, which resulted in the discontinuity between the conductive zones C3 (also C4) and C1 (Figure 3).
(3) Because of the thermal insulation of the subducted Indian plate, the thermal sources of hot springs in the Dinggye region and surroundings are derived from the radioactive thermal in the upper crust and the thermal conduction of the southern migration of the crustal materials, which also corresponds with the crust-derived Helium within.
(4) Combined with the electrical structure in the Ranba region (Yadong-Gulu rift; Wei et al., 2001; Figure 4) and Woka region (Riduo-Cona rift; Xue et al., 2022; Figure 4), we indicate that the rheological variation of the upper crust resulted from the southern migration of the lithospheric materials is an important reason of the formation of the N-S-direction rifts in the Tethys-Himalaya terrane (Figure 5).

Acknowledgements

This study is funded by the National Key R&D Program of China (2022YFF0800901), the Second Tibetan Plateau Scientific Expedition and Research Program (STEP) (2019QZKK0701), China Scholarship Council (202006400054).

References

Chen, J., Gaillard, F., Villaros, A., et al., 2018. Melting conditions in the modern Tibetan crust since the Miocene. Nature Communications, 9, 1-13. DOI: 10.1038/s41467-018-05934-7

Egbert, G.D., and Kelbert, A., 2012. Computational recipes for electromagnetic inverse problems. Geophysical Journal International, 189(1), 251-267. DOI: 10.1111/j.1365-246x.2011.05347.x

Kelbert, A., Meqbel, N., Egbert, G. D., and Tandon,

K., 2014. ModEM: a modular system for inversion of electromagnetic geophysical data. Computers & Geoscience, 66, 40-53. DOI: 10.1016/j.cageo.2014.01.010

King, J., Harris, N., Argles, T., et al., 2011. Contribution of crustal anatexis to the tectonic evolution of India crust beneath southern Tibet. Geological Society of America Bulletin 123, 218–239. DOI: 10.1130/B30085.1

Sheng, Y., Jin, S., Comeau, M. J., et al., 2021. Lithospheric structure near the northern Xainza-Dinggye Rift, Tibetan Plateau – implications for rheology and tectonic dynamics. Journal of Geophysical Research: Solid Earth. DOI: 10.1029/2020JB021442

Unsworth, M. J., Jones, A. G., Wei, W., et al., 2005. Crustal rheology of the Himalaya and southern Tibet inferred from magnetotelluric data. Nature, 438(7064), 78-81. DOI:10.1038/nature04154

Wei, W., Unsworth, M., Jones, A., et al., 2001. Detection of widespread fluids in the Tibetan crust by magnetotelluric studies. Science, 292(5517), 716-9. DOI:10.1126/science.1010580

Xue, S., Lu, Z. W., Li, W. H., et al., 2022. Electrical resistivity structure beneath the central Cona-Oiga rift, southern Tibet, and its implications for regional dynamics. Earth Science Frontiers, 29(2): 393-401. DOI: 10.13745/j.esf.sf.2022.2.3

Yu, J. J., Zeng, L. S., Liu. J., et al., 2011. Early Miocene leucogranites in Dinggye area, southern Tibet: Formation mechanism and tectonic implications. Acta Petrologica Sinica，27(7):1961-1972

Zhang, Z. M., Kang, D. Y., Ding, H. X., et al., 2018. Partial melting of himalayan orogen and formation mechanism of leucogranite. Earth Science (Abstract in English), 43(1), 17. CNKI:SUN:DQKX.0.2018-01-007.

Figures, Tables and Equations

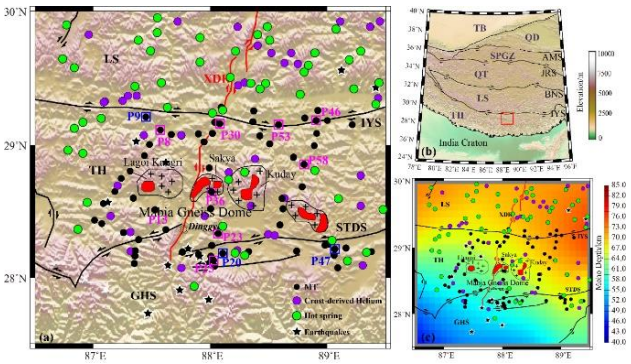

Figure 1. Map of the study area in the vicinity of the Dinggye region, Central Himalaya. (a) Map showing the locations of MT measurement sites (black dots) used in the study. Also shown are major tectonic structures (faults and sutures in black, rifts in red; from Bian et al., 2018, and Wang et al., 2017), crustal helium (purple dots; Hou et al., 2004; Klemperer et al., 2022), intermediate-depth earthquakes at 65-100 km depth (stars; Klemperer et al., 2022), hot springs (green dots; Klemperer et al., 2022),and the areas Lhagoi, Sakya, and Kuday that belong to the Mabja Gneiss Dome (areas marked with cross symbols and red (leucogranite core); Langile et al., 2010; Xue et al., 2022). Pink rectangles are the selected MT stations in Figure 3. (b) Regional map of the Tibetan Plateau and surroundings showing tectonic features. The red rectangle outlines the study area. (c) Map of the Moho depth in the survey area determined with seismic measurements (Li et al., 2013). XDR: Xainza-Dinggye Rift; GHS: Greater Himalaya Sequence; STDS: Southern Tibetan Detachment System; TH: Tethys–Himalaya; LS: Lhasa terrane; QT: Qiangtang terrane; IYS: Indus–Yarlung Zangbo suture; BNS: Banggong–Nujiang suture; JRS: Jinsha River suture; AMS: Animaqing suture; SPGZ: Songpan–Ganzi basin; QD: Qaidam basin; TB: Tarim basin

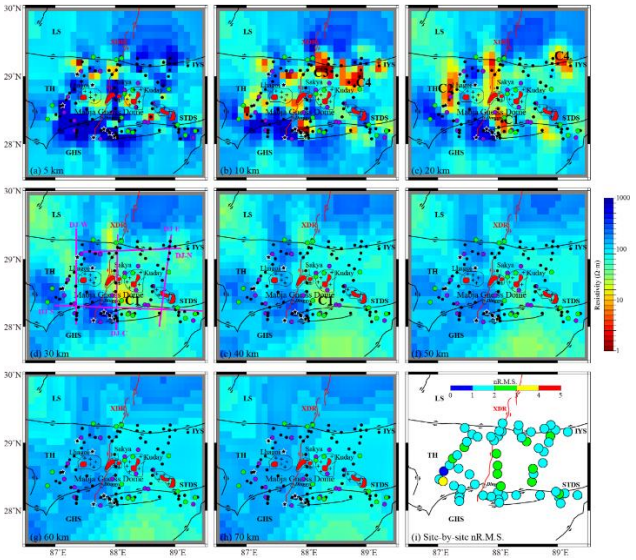

Figure 2. Horizontal slices of the 3-D electrical resistivity model. (a) – (h) Depths of 5, 10, 20, 30, 40, 50, 60 and 70 km, respectively. C1, C2, C3 and C4 mark the conductive zones. (i) The site–by–site nR.M.S. misfit of the 3-D inversion. See Figure 1 for labels. The pink lines indicate the profiles.

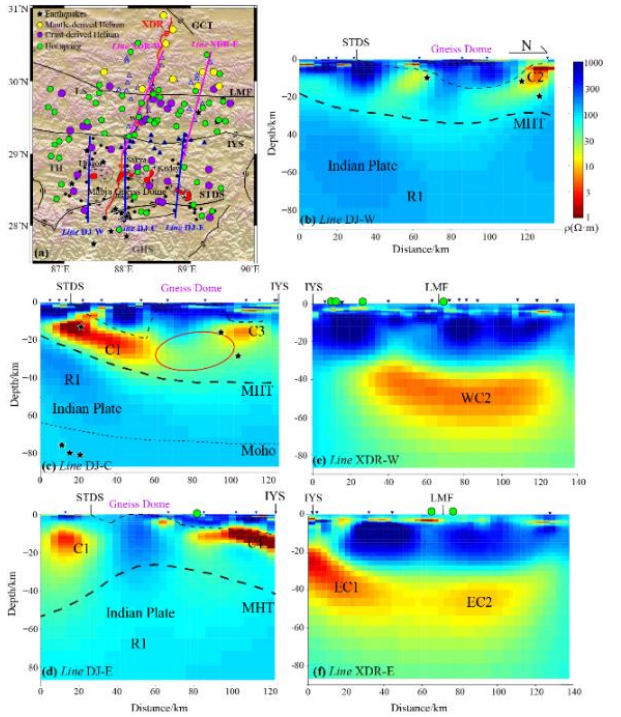

Figure 3. Vertical cross sections, in the south-north direction, of the 3-D electrical resistivity models.

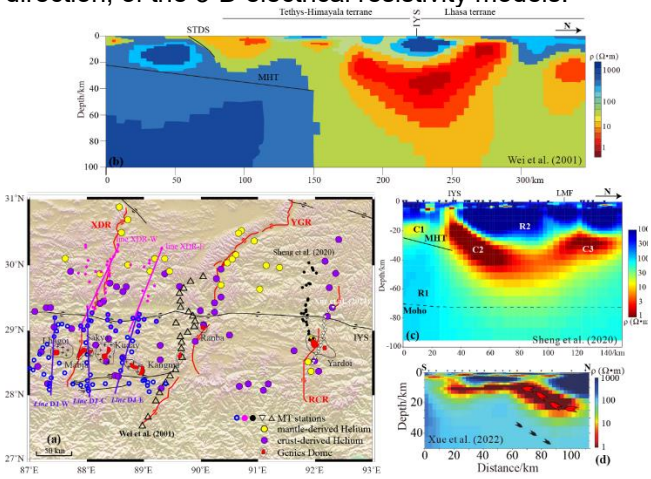

Figure 4. Electrical resistivity models in the vicinity of the YGR and RCR. (a) Map of the region. The locations of MT measurement sites are indicated (this study, blue circles; Sheng et al., 2021, pink dots; Wei et al., 2001, black triangles; Sheng et al., 2020, black dots; Xue et al., 2021, white dots). The various rift zones are marked with red lines. Gneiss Domes across the region are marked (cross symbols and red). (b) Electrical resistivity model of Xue et al. (2022). (c) Electrical resistivity model of Sheng et al. (2020). (d) Electrical resistivity model of Wei et al. (2001). Areas Ranba, Kangma and Yardoi are Gneiss Domes in the Tethys-Himalaya terrane, east of the Mabja complex. Yadong-Gulu rift = YGR. Riduo-Cuona rift = RCR.

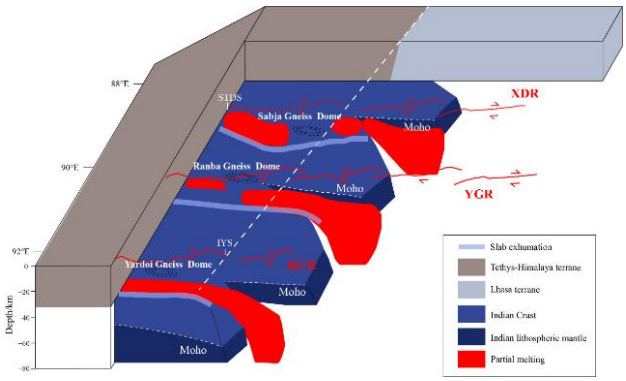

Figure 5. Cartoon sketch of the tectonic–dynamic process in the eastern Himalayan orogenic belt. Red regions may represent material and fluid migration from the middle-lower crust to the upper crust. Black dotted circles represent the Mabja, Ranba and Yardoi gneiss domes in the Northern Himalaya Gneiss Dome belt (near longitudes of approximately 88°E, 90°E, and 92°E). White dashed lines indicate the Moho depth.